




Binder jetting in gears

Process design and tooth bending strength for gears made of 17-4PH

Lukas Klee¹  · Thomas Bergs¹ · Mareike Solf¹ · Jens Brimmers¹

Received: 14 March 2023 / Accepted: 27 April 2023 / Published online: 12 June 2023
© The Author(s) 2023

Abstract

Due to near netshape production, powder metallurgically manufactured (PM) gears have a high potential to increase cost and resource efficiency. Compared to conventionally machined gears, the advantages of PM gears are the different local density distribution in the component and the potential integration of secondary design elements. These advantages are accompanied by the reduction of weight and the possibility of optimizing the NVH-behavior of a gear. PM gears may be manufactured by both, die pressing and additive manufacturing (AM). The powder bed-based additive manufacturing processes for metals can be classified into binder-based (e.g. Binder Jetting, BJT) and beam-based thermal processes (e.g. Laser Powder Bed Fusion, LPBF). Due to the specific process technology, the manufacturing of PM gears by die pressing is only economical for large batch sizes in series production. For small batches, AM offers an approach to manufacture gears that meet the requirements in terms of quality, strength, acoustics and economic efficiency of the manufacturing process.

This report describes the potential of BJT gears made of stainless steel 17-4PH (X5CrN-CuNb16-4) with a relative density of $\rho_{0,rel} \approx 99\%$ regarding the tooth bending strength. The reliability of the process and thus the tooth bending strength can be increased further by a specific adjustment of process parameters. Subsequently, the gears are tested with regard to the tooth bending strength on the pulsator test rig. The results are summarized in a SN-curve.

✉ Lukas Klee
l.klee@wzl.rwth-aachen.de

¹ Laboratory for Machine Tools and Production Engineering (WZL), Gear Department, Chair of Manufacturing Technology, RWTH Aachen University, Campus-Boulevard 30, 52074 Aachen, Germany

Binder Jetting von Verzahnungen

Prozessoptimierung des Binder Jettings von Zahnrädern aus 17-4PH unter Berücksichtigung der Zahnfußtragfähigkeit

Zusammenfassung

Pulvermetallurgisch (PM) hergestellte Zahnräder weisen aufgrund der endkonturnahen Fertigung ein hohes Potenzial zur Steigerung der Kosten- und Ressourceneffizienz auf. Vorteile pulvermetallurgisch hergestellter (PM) Zahnräder sind die im Vergleich zur konventionellen subtraktiven Fertigung durch den Sinterprozess einstellbare Bauteildichte und die mögliche Integration von sekundären Konstruktionselementen. Diese Vorteile induzieren eine Gewichtsreduktion sowie mögliche Optimierung des „Noise Vibration Harshness“ (NVH) Verhaltens der Zahnräder. Pulvermetallurgische Zahnräder können sowohl mittels Matrizenpressen als auch additiver Fertigung (Additive Manufacturing, AM) gefertigt werden. Die pulverbettbasierten additiven Fertigungsverfahren für Metalle werden in binderbasierte (z. B. Binder Jetting, BJT) und strahlenbasierte, thermische Verfahren (z. B. Laser Powder Bed Fusion, LPBF) unterteilt. Die Herstellung pulvermetallurgischer Zahnräder durch Matrizenpressen ist aufgrund der speziellen Anlagentechnik erst bei großen Losgrößen bzw. in der Serienfertigung wirtschaftlich. Mit additiven Fertigungsverfahren soll die Fertigung von Zahnrädern in Kleinserie ermöglicht werden, durch welche die Anforderungen hinsichtlich Wirtschaftlichkeit, Qualität, Festigkeit und Akustik umsetzbar sind.

In diesem Bericht wird das Potenzial von Binder Jetting Zahnrädern aus dem Werkstoff 17-4PH (Edelstahl X5CrNiCuNb16-4) bei einer relativen Dichte von $\rho_{0,rel} \approx 99\%$ hinsichtlich der Zahnfußtragfähigkeit beschrieben. Durch eine gezielte Anpassung von Prozessparametern beim Binder Jetting wird die Prozessstabilität und damit einhergehend die Zahnfußtragfähigkeit weiter gesteigert. Sowohl die Zeit- als auch die Dauerfestigkeit der BJT Zahnräder aus dem Werkstoff 17-4PH werden untersucht und die Ergebnisse in einem Wöhlerdiagramm zusammengefasst.

1 Introduction and motivation

Due to near netshape production, powder metallurgically manufactured (PM) gears have a high potential to decrease costs and increase resource efficiency. Compared to conventionally machined gears, the advantages of powder metallurgically manufactured (PM) gears are the different local density distribution in the component and the potential integration of secondary design elements. These advantages are accompanied by the reduction of weight and the possibility of optimizing the NVH-behavior of a gear [24]. Due to the expected future shift of the automotive industry from combustion engines to electrified powertrains, the optimization of the noise behavior of transmission components is becoming increasingly important [28]. Powder metallurgical gears may be manufactured by both, die pressing and additive manufacturing (AM). The powder bed-based additive manufacturing processes for metals can be classified into binder-based (e.g. Binder Jetting, BJT) and beam-based thermal processes (e.g. Laser Powder Bed Fusion, LPBF). Due to the specific process technology, the manufacturing of PM gears with die pressing is only economical for large batch sizes in series production. For small batches, additive manufacturing offers an approach to manufacture gears that meet the requirements in terms of quality, strength, acoustics and economic efficiency of the manufacturing process.

Additively manufactured products contribute to increasing individualization and variety, as undercuts and functional elements can be integrated directly into the component. These can only be integrated into the design using

additive manufacturing processes due to the additional degrees of freedom. The achievable geometric complexity in the design offers new possibilities for use and optimization and requires increasing flexibility in manufacturing [5].

This report describes the potential of BJT gears made of stainless steel 17-4PH (X5CrNiCuNb16-4) with a relative density of $\rho_{0,rel} \approx 99\%$ in terms of tooth bending strength. The reliability of the process and thus the bending strength of the teeth can be further increased by specific adjustment of the Binder Jetting process parameters. Both endurance and fatigue strength of 17-4PH BJT gears are investigated and the results are summarized in a SN-curve. In addition, the endurance strength of cold rolled gears made of 17-4PH ($\rho_{0,rel} \approx 93.98\%$) is determined in screening tests and evaluated by comparison with load capacity results of densified gears made of 316L (stainless steel X2CrNiMo17-12-2). In this case, the development of the process parameter is not part of this report.

2 Manufacturing of binder jetting gears considering the tooth bending strength

Binder Jetting (BJT) of gears is a multi-stage additive manufacturing process. The components are produced in two or more operations [9]. The BJT process produces green compacts of gears which are sintered by secondary heat treatment processes. During the sintering process, the powder particles form a diffusion bond [3], the porosity decreases and the component volume shrinks [21]. Both the pow-

der mixture and the binder are prepared according to the defined recipe. Subsequently, the “printing”, the layer-by-layer generation of the green gear, takes place by applying the liquid organic binder locally to the powder bed (build-box) and bonding both the powder particles and the existing layers together. Since no additional heat is generated during the production process, it does not have to be dissipated via specific constructions. After the printing process, the binder is cured. For this purpose, the entire buildbox is moved into the curing oven with the printed gears and the unused, recyclable powder. Afterwards the gears are removed from the powder bed. Afterwards, the binder is removed from the produced green gears by a thermal treatment. The following sintering and heat treatment process produces the final strength and densifies the green gears by shrinkage. After the heat treatment steps, the gear is transformed into a purely metallic state [2]. The material powder used for additive manufacturing must have good flowability as well as a high filling density [3]. To date, commercial systems mainly process stainless steels (316L, knife steel 420, 17-4 PH) as well as titanium alloys such as Ti6Al4V and copper [2, 4, 12, 15]. In the following, previous investigations on the Binder Jetting of gears made from stainless steels 316L and 17-4PH are described.

2.1 Gears made of stainless steel 316L

Initial investigations on the manufacturing of gears using BJT as well as the analysis of the tooth bending strength were conducted with the material 316L (stainless steel X2CrNiMoN17-12-2). This metallic material is certified and established for the binder jetting process [2]. The gears were sintered after printing with regard to a relative core density of $\rho_{0,rel} \approx 92\%$. In analogy to the process chain of die pressing in series production, the near surface zone of the BJT gears is compacted by densification rolling using the machine PROFIROLL PR 15HP. The material 316L shows ductile properties and therefore can be cold-formed without problems [26]. After manufacturing, both the fatigue strength and the endurance strength of the gears were analyzed. The results were summarized in a SN-curve. The experimental investigations of the ground gears were performed on a pulsator test rig. With regard to the fatigue strength, the endurable double amplitude as well as the tooth root stress were determined. The mean value of the endurable double amplitude ($N_G = 3 \cdot 10^6$ LC) was $2 \cdot F_{A,mean} = 6.26$ kN, corresponding to an endurable tooth root stress of $\sigma_{F0} = 351.14$ N/mm² calculated according to ISO 6336-3 [17]. This value of the double amplitude corresponds to the fatigue strength characteristic value for a failure probability of $P_a = 50\%$. The intersection of the endurance and fatigue lines was located at the double amplitude force of $2 \cdot F_{A,mean} = 6.26$ kN and the number of

load cycles of $N = 1,940,000$. Both within the test points of a gear and within the BJT batch, there was hardly any variation in the results and load cycles achieved. The reproducibility of the results verifies the suitability of BJT in gear production for the first time [20]. A pressed and sintered gear made of the material Fe + 0.85% Mo + 0.25% C was tested as a reference on the pulsator test rig. The mean value of the endurable double amplitude ($N_G = 3 \cdot 10^6$ LC) was $2 \cdot F_{A,mean} = 8$ kN [20]. Comparable studies regarding the tooth bending strength of Binder Jetting gears should be conducted with a certified metallic material, which has significantly higher strength values and therefore implies a higher tooth bending strength.

2.2 Gears made of stainless steel 17-4PH

The material 17-4PH (stainless steel X5CrNiCuNb16-4) has a significantly higher mechanical strength compared to 316L and thus implies an increase in the tooth bending strength of the manufactured gears [1, 6, 8]. Compared to the BJT gear production from the material 316L, a new design of the BJT process parameters is essential due to different material characteristics. The impact of different process variations along the process chain of BJT gears made of the material 17-4PH was investigated [19]. During the printing process of the green gear, the powder and binder application have been identified as the main influencing factors on the final print result. The most relevant variables for powder application are the layer thickness D_s , as well as the application direction and speed v_p as a function of the processed material powder [19]. When applying powder in two directions, a larger amount is introduced into the powder bed at a constant layer thickness D_s and thus the density of the green gear increases. A higher green density implies a lower shrinkage during sintering. This results in a reduction of the induced stresses and a decrease in crack formation [19]. Subsequently, support structures for gear manufacturing by means of BJT were discussed, which are particularly relevant for the subsequent post-treatment processes curing and sintering to minimize the risk of fracturing. Structural support structures correspond to small components that are additionally produced with the gear in a printing process. While curing, the stresses are induced by the static and dynamic interactions of the powder. The process stability of debinding and sintering was significantly increased by the use of a mesh disk between the gear and the ceramic sintering base [19]. Effects of the sintering furnace on the printing result, especially if a retort furnace is used, also have to be considered. The identified process parameters are summarized in Fig. 1.

When powder was applied in two directions (outward and backward path above the buildbox) at a constant powder application speed $v_p = 50$ mm/s, the amount of applied

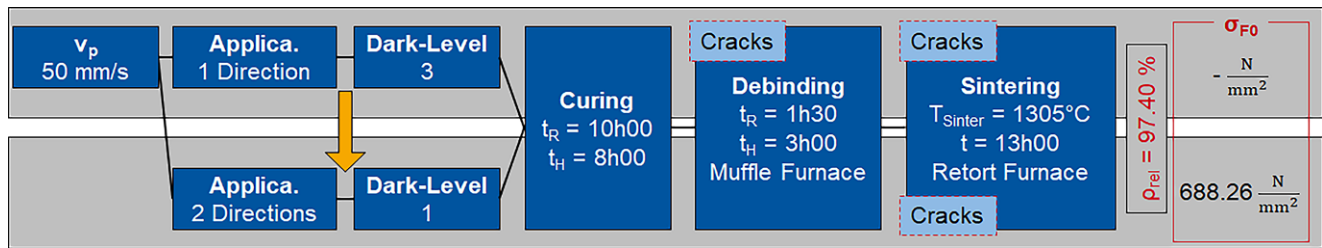


Fig. 1 Initial process parameters for the production of BJT gears from 17-4PH

binder (Dark-Level) was reduced. In addition to the optimizations in powder application, the part quality can be further increased by adjusting the control variables for binder application. Basically, the binder is applied to the BJT system DM P2500 via two cartridges. The amount of binder applied can be adjusted by varying the number of nozzles (number of pixels) of the respective cartridge. The green gear geometry is described in the layer by pixels. Thus, pixels can be eliminated from the binder application based on defined patterns, similar to that of a chessboard. At least 50% of all pixels (Dark 0) of a component geometry must be printed. Dark Level 1 corresponds to 55.56% of the maximum amount of binder that can be applied, Dark Level 3 to 66.67% and Dark Level 8 to the maximum amount of binder (100%). During curing, the buildbox with the printed gears and the unused, recyclable powder is heated from ambient temperature to the curing temperature $T_C = 200^\circ\text{C}$ over a defined period of time t_R (ramp time) immediately after printing. Afterwards the gears remain in the oven at the temperature T_C for a calculated holding time t_H . The process times in the oven can be calculated by the amount of binder used during printing and the number of layers. Thus, the times are varying for each print. When simultaneously printing four gears made of material 17-4PH, the ramp time is approximately $t_R = 10\text{h}$ and the holding time at T_C is approximately $t_H = 8\text{h}$. Debinding was realized in a muffle furnace and sintering in a retort furnace. The relative density of the gears made of the material 17-4PH after sintering was $\rho_{0,\text{rel}} \approx 97.4\%$ [19].

Despite the process modifications explained previously, some of the gears cracked depending on their position in the furnace after sintering (cf. Fig. 1, bottom right). Thus only a screening could be conducted to investigate the tooth bending strength. In addition, an uneven grinding allowance respectively undersize on the flanks was detected. The mean value of the endurable double amplitude ($N_G = 3 \cdot 10^6$ LC) of the BJT gears was $2 \cdot F_{A,\text{mean}} = 10.60\text{kN}$, corresponding to an endurable tooth root stress of $\sigma_{F0} = 688.26\text{N/mm}^2$. The comparison with load capacity results of densified gears made of 316L (stainless steel X2CrNiMo17-12-2) showed an increase of almost 95% [20].

3 Objective and approach

The additive manufacturing process of Binder Jetting is intended to enable the production of individualized gears in small batch sizes, through which all requirements with regard to quality, strength, acoustics and cost-effectiveness can be implemented. The objective of this report is to optimize the process for gear manufacturing using 17-4PH (stainless steel, X5CrNiCuNb16-4), see Fig. 2. The evaluation is based on the one hand on the process-reliable reproducibility of the gears and on the other hand on the resulting tooth bending strength. Proceeding from the knowledge already developed for gear production from the material 17-4PH at a relative component density $\rho_{0,\text{rel}} \approx 97.4\%$ —production and use of support structures, knowledge of the main factors influencing the final print result, as well as initial process parameters along the process chain—the reliability of the process and thus the tooth bending strength is increased through a specific adjustment of the process parameters. Both the endurance strength and the fatigue strength of the BJT gears made of material 17-4PH are analyzed and the results are summarized in a SN-curve, see Fig. 2.

Due to already established results on the tooth bending strength of cold rolled gears made of the material 316L [20], gears are manufactured of 17-4PH with an allowance for densification ($\rho_{0,\text{rel}} \approx 93.98\%$) for screening tests. The densification of the surface zone by the rolling results in a graduation of the density from the surface to the core. Subsequently, the gears are examined in screening tests with regard to the tooth bending strength on the pulsator test rig. Thus, in this report describes the influences of relevant process parameters on the component properties and the tooth bending strength of the gears.

4 Gear manufacturing with optimized process parameters

Based on the process parameters developed in Chap. 2, further modifications to the process were necessary for a reliable and reproducible production of BJT gears made of 17-4PH. Modifications were made regarding the powder appli-

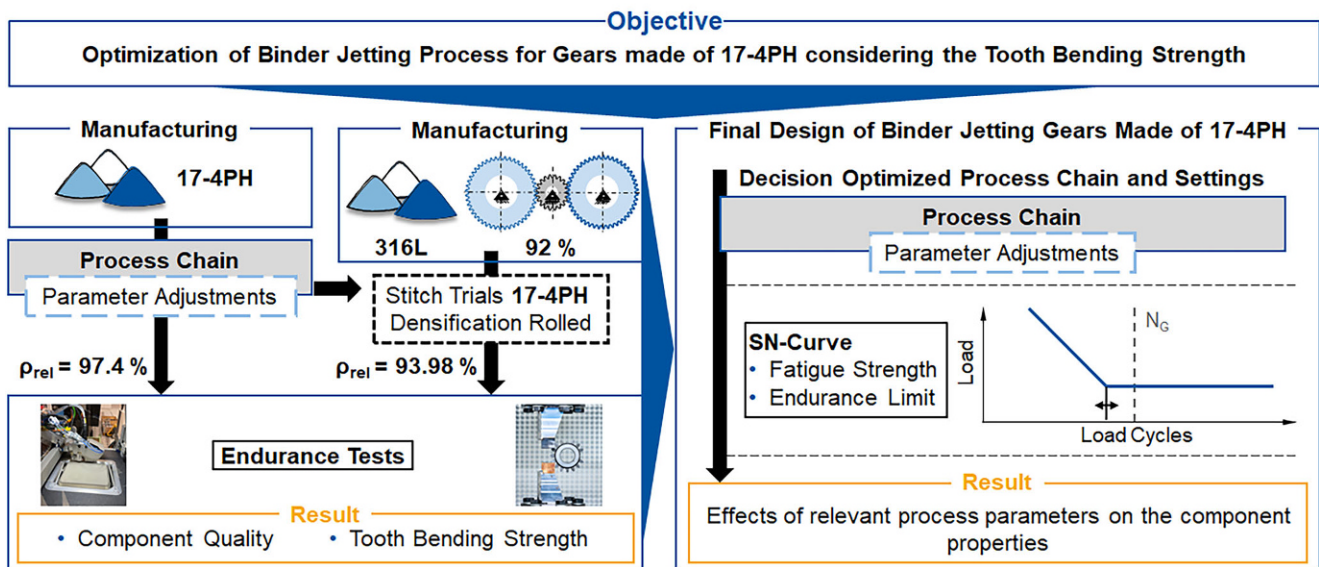


Fig. 2 Objective and Approach

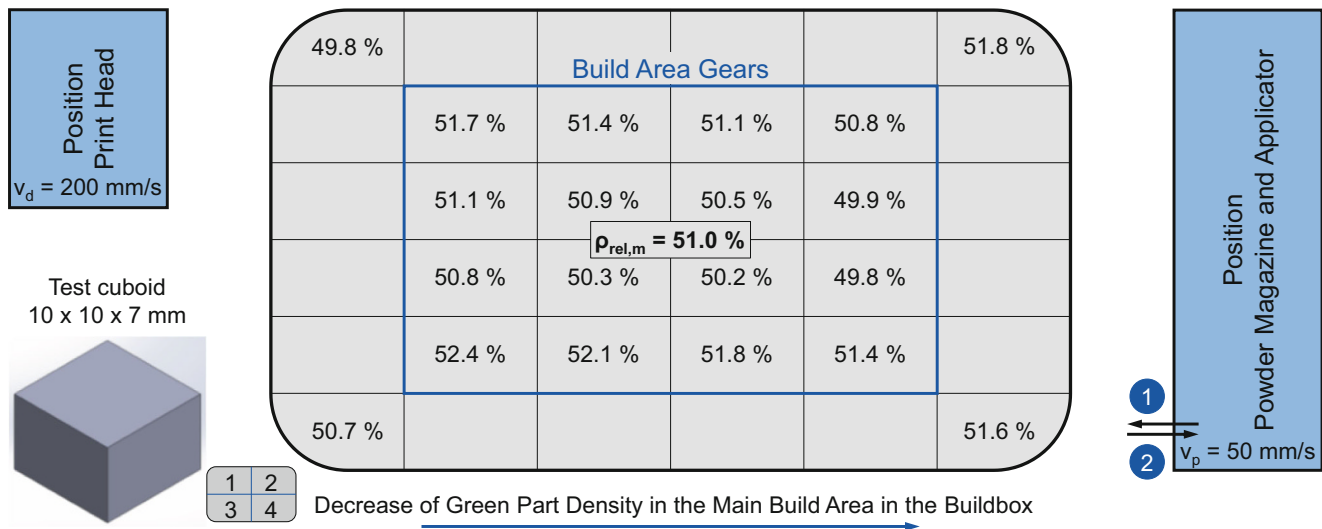


Fig. 3 Relative Green Density in the Buildbox

ation, the component scaling and thus the curing process as well as the debinding and sintering process. Before testing, the gear quality and the surface roughness of the BJT gears were measured.

Powder application The previous occurrence of crack formations at some gears could result from variations in the relative green densities depending on the positioning in the powder bed. Generally, a cube (measuring 10×10×7 mm) was produced in each of the four corners of the build box for the previous print jobs. As the volume of the cubes and the density of the material 17-4PH were known, the relative green density could be calculated. The relative green density of the previously manufactured gears var-

ied in a range of $\Delta\rho_{rel}=2.2\%$ based on the four cubes. In addition, only low values of the relative green density were obtained in the lower limit of the desired range of $\rho_{rel}=50\text{--}60\%$. For the analysis of the relative green density distribution over the entire powder bed and thus in the printing area of the gears, 16 further test cubes, distributed in the buildbox, were manufactured subsequently, cf. Fig. 3. Printing was done with the process parameters deduced in Chap. 2: powder application in two directions of motion, 56.26% of all pixels were wetted with binder (Dark Level 1), layer thickness of $D_s=42\mu\text{m}$, powder application speed $v_p=50\text{mm/s}$ and binder application speed of $v_d=200\text{mm/s}$. The average value of the relative green density of the cubes was $\rho_{rel,min}=49.8\%$ and the maximum

density was $\rho_{\text{rel,max}} = 52.4\%$. The decrease of the green density in the powder bed from the print head side to the powder magazine side was notable. The decrease was approximately $\Delta\rho_{\text{rel}} = 1\%$. In addition to powder application in two directions of motion, the reduction of the powder application speed v_p is another possibility to increase and stabilise the green density. A higher green density implies a lower shrinkage during sintering. This results in a reduction of the induced stresses and a decrease in crack formation. The application speed was therefore reduced to $v_p = 40 \text{ mm/s}$ while the layer thickness D_s was kept constant. Hence, a larger quantity of powder is inserted into the powder bed, the green density increases further. However, the productivity decreases. After reducing the application speed v_p , an average green density of $\rho_{\text{rel,m}} = 53.4\%$ was reliably achieved during the process. The determined average density of green gears was assumed to be sufficient for the following prints. It could be kept constant in the range of $\Delta\rho_{\text{rel}} = 1.7\%$ over all gear prints conducted.

Scaling of the gear and thermal processes After sintering the gears, the geometric analysis revealed a partial undersize on the flanks and thus an insufficient grinding allowance. Therefore, the scaling factors of the printed gear were increased in X-, Y- and Z-direction ($\Delta = 3.43\%$) to prevent sintering shrinkage, see Fig. 4.

The adjustment of the scaling factors leads to an increasing amount of binder during printing and thus an extension of the curing process. When simultaneously printing four gears made of material 17-4PH, the increased amount of binder resulted in a ramp time of approximately $t_R = 11 \text{ h } 30 \text{ min}$. The holding time at T_C kept constant at $t_H = 8 \text{ h}$. Based on the previous experience of debinding in a muffle furnace and sintering in a retort furnace, the gears were debinded and sintered at identical process conditions in a continuous furnace using a protective gas atmosphere (hydrogen H_2). After sintering, no visible damage or cracks at the gears was detected. 16 gears has been printed. All of them had sufficient oversize and a relative density of $\rho_{\text{rel}} = 99\%$. The resulting relative density was higher than the relative

density of the variant tested in the screening trials [19]. Thus, the type of sintering furnace has a significant influence on the final component quality. The previously developed mesh disc was used as a support structure during sintering.

Hard machining The BJT gears were profile ground using a KAPP KX 500 FLEX gear grinding machine. Due to the partially high allowance in the area of the tooth root and tooth tip, cf. Fig. 4, the final geometry was produced in two roughing and one finishing cut to avoid grinding burn. The gear quality was measured on a KLINGELNBERG P65 gear measuring machine. The measurement was conducted on all gears in order to achieve the best possible statistical validation of the evaluation. In addition to the profile and helix deviation, the single and accumulated pitch errors f_p as well as the radial runout error F_R were measured. All measured values of the BJT gears averaged minimum within IT5 according to DIN EN ISO 1328 [7].

The surface roughness of the respective tooth profiles of the BJT gears was measured after grinding using the tactile roughness measuring device HOMMEL ETAMIC NANOSCAN 855. The evaluation of the roughness values and measurement reports was performed in accordance with DIN EN ISO 21920-3 in the direction of the profile [10]. In total, six roughness measurements were performed for each gear. Of four teeth evenly distributed over the circumference, a roughness measurement was taken on both the right and the left flank of the respective tooth. The mean value of all R_z measurements (maximum height of the roughness profile) after hard finishing was $R_z = 2.3 \mu\text{m}$, the arithmetic average roughness value $R_a = 0.3 \mu\text{m}$. The roughness of the ground tooth roots of all the gears examined was within this range as well.

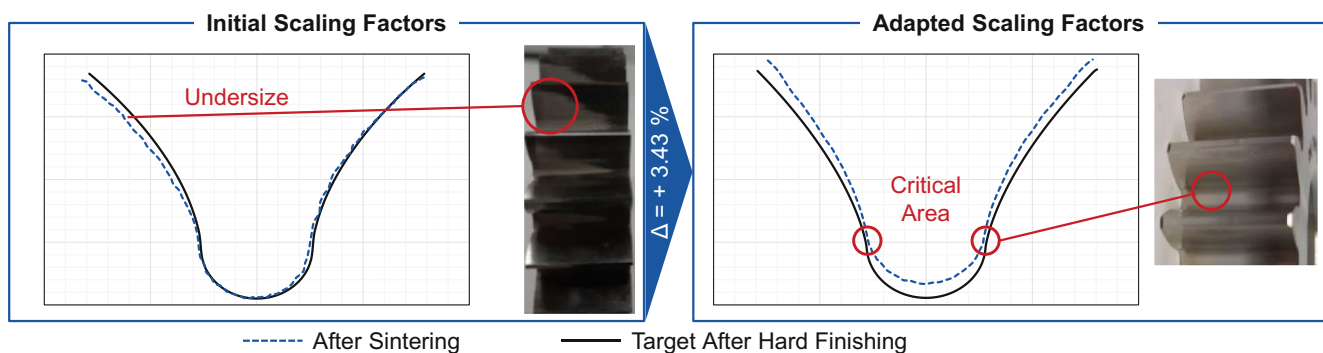


Fig. 4 Tooth Space before and after adjusting the scaling factors

5 Validation of the binder jetting process chain regarding the tooth bending strength

The following chapter describes the results of the tooth bending strength tests of the additively manufactured BJT gears ($\rho_{0,rel} \approx 99\%$). The results are summarized in a SN-curve. Furthermore, in analogy to the results already obtained on the tooth bending strength of cold rolled gears made of 316L [20], gears were manufactured from 17 4PH with an allowance for cold rolling (relative core density $\rho_{0,rel} \approx 93.98\%$). The gears were classified in the state of the art by comparison with cold rolled gears made of 316L.

5.1 Experimental design and description

Gear-critical load types are stresses on the tooth flank due to rolling and bending fatigue in the tooth root [13, 23, 27]. The experimental investigations of the ground gears with regard to the tooth bending strength were performed on a pulsator test rig. The pulsator is an analogy test rig which approximates a part of the stress curve occurring in tooth meshing with an alternative concept of load application, see Fig. 5. According to the definition of the ISO 6336-3 standard, the tensile and compressive stresses σ_Z and σ_D resulting from the mechanical load reach the maximum at the tooth root in the area of the 30° tangent [17].

The main advantage of the pulsator test compared to the running test is the possibility of multiple use of a gear. In addition, no counter gear is required. The number of possible test points depends on the contact line to be examined and the number of teeth z_2 of the gear. The BJT gear contains four test points. The gear is clamped over several teeth between two plane-parallel pulsator clamps—four

teeth are clamped at the BJT gear. The tooth normal force from the running test is applied to the gear. One clamp performs an oscillating movement and, in this way, introduces a sine-shaped force curve into the tooth. The other stationary clamp absorbs the applied force. The force applied is monitored and controlled by using a load cell.

5.2 Investigation of the tooth bending strength

In order to describe the component characteristics, 10 tests were performed in the endurance strength load range using the stair-step method [29] on two load levels. Another 14 tests were conducted at the transition to the fatigue strength load range using the stair step method [11]. The stair step method was evaluated according to HÜCK [16]. The load step of the endurance limit of the BJT gears is shown in Fig. 6.

The fictitious point formed the 15th test point. The load step increase per double amplitude was $\Delta 2 \cdot F_A = 1 \text{ kN}$. The ratio of a load step to the standard deviation was approximated according to HÜCK [16]. The limiting number of oscillations for the tooth bending strength is set to $N_G = 3 \cdot 10^6$ load cycles (LC) according to ISO 6336 part 3 [17]. Termination criteria during the pulsator test are reaching the limit number of load cycles and tooth root fracture [22]. According to the HÜCK staircase method, the following test depends on the previous test result. In the case of a tooth root fracture before reaching the limit number of load cycles N_G , the load or the stress is reduced by one step ($\Delta 2 \cdot F_A = 1 \text{ kN}$). Otherwise, in the case of a run-out, the load or the stress is increased by one step [11]. The Y-axis (Fig. 6) shows on the one hand the force $2 \cdot F_A$ of the double amplitude, which indicates the stress range, and on the other hand the tooth root stress σ_{F0} calculated accord-

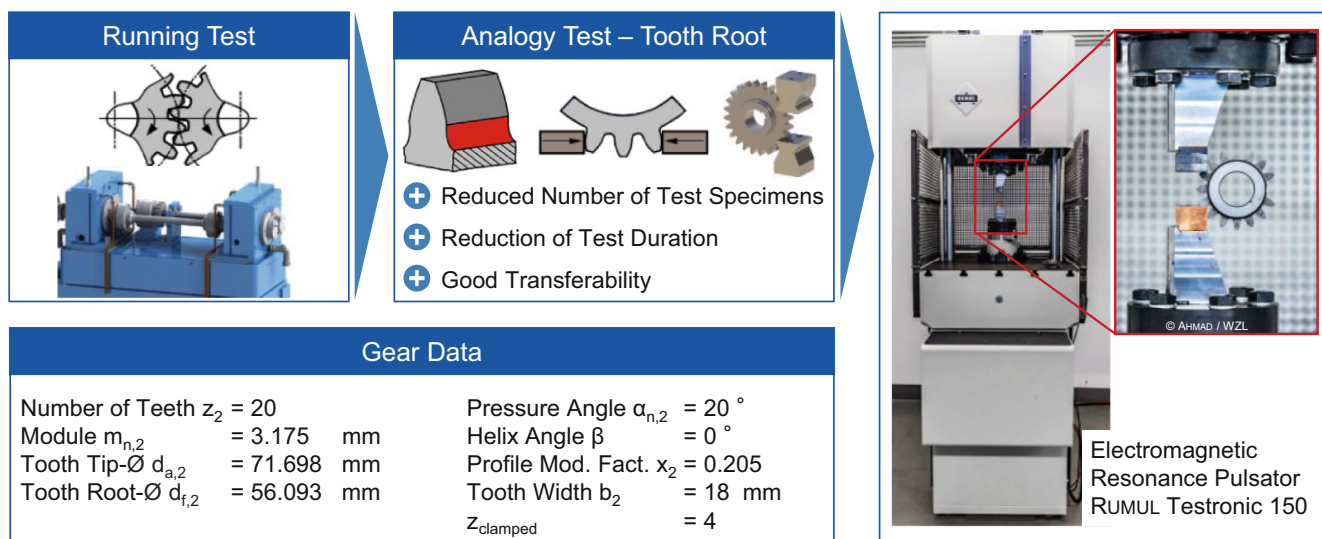


Fig. 5 Analogy test for determining the tooth root load capacity

Test Conditions

- F_o = -0.5 kN
- F_u = variable
- F_A = variable
- f_{p4} ≈ 153 Hz
- $z_{clamped}$ = 4
- P_a = 50 %
- T ≈ RT (21°C)
- LC = Load Cycles

Pulsator Test Rig

- P4: Electromagnetic Resonance Pulsator RUMUL TESTRONIC 150

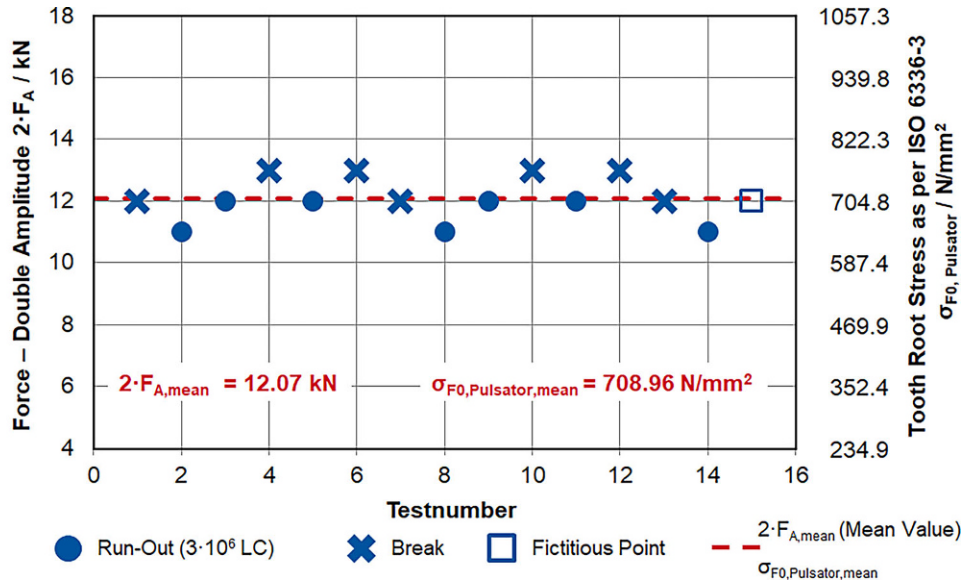
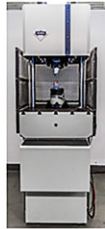


Fig. 6 Endurance Limit for BJT gears made of 17-4PH ($\rho_{rel} = 99.0\%$) according to HÜCK [16]

Test Conditions

- F_o = -0.5 kN
- F_u = variable
- F_A = variable
- f_{p4} ≈ 153 Hz
- $z_{clamped}$ = 4
- P_a = 50 %
- T ≈ RT (21°C)
- LC = Load Cycles

Pulsator Test Rig

- P4: Electromagnetic Resonance Pulsator RUMUL TESTRONIC 150

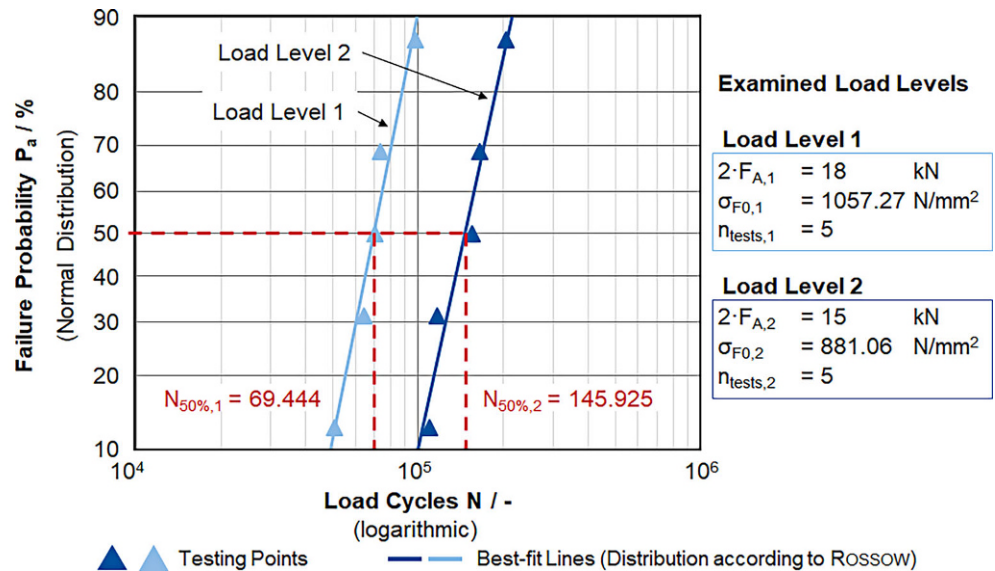


Fig. 7 Fatigue Strength of the BJT gears (17-4PH, $\rho_{rel} = 99.0\%$) according to the Horizon Method

ing to ISO 6336 part 3 [17]. The tooth root stress describes the local load in the tooth root. The test frequency of the pulsator test rig was $f_{p1} = 143$ Hz and thus below the critical test frequency of $f_{crit} = 200$ Hz, below which no influences of the test frequency on the results are to be expected [18]. The mean value of the endurable double amplitude ($N_G = 3 \cdot 10^6$ LC) was $2 \cdot F_{A,mean} = 12.07$ kN, corresponding to an endurable tooth root stress of $\sigma_{F0} = 708.96$ N/mm². The mean value of the double amplitude corresponds to the endurance strength characteristic value for a failure probability of $P_a = 50\%$. The standard deviation was $s = 2\%$.

To determine the fatigue strength ($N_G < 3 \cdot 10^6$ LC), a defined number of tests were performed according to the hori-

zon method at two different load levels [25]. The difference between the two load levels should be as large as possible in order to be able to make the best possible estimation of the fatigue strength line with regard to its slope and position. The minimum number of tests should be five [29]. Five test runs were performed at both tested load levels of $2 \cdot F_{A,1} = 18$ kN as well as $2 \cdot F_{A,2} = 15$ kN, see Fig. 7.

The corresponding load cycles N of each test were ranked in increasing order on the respective load level. For each test point, the probability of failure P_a was calculated based on the logarithmic normal distribution according to ROSSOW's method [14, 25]. After transferring the paired values of probability of failure P_a (Y axis) and number of

Test Conditions

- F_o = -0.5 kN
- F_u = variable
- F_A = variable
- f_{p4} \approx 153 Hz
- $z_{clamped}$ = 4
- P_a = 50 %
- T \approx RT (21°C)
- LC = Load Cycles

Pulsator Test Rig

- P4: Electromagnetic Resonance Pulsator RUMUL TESTRONIC 150

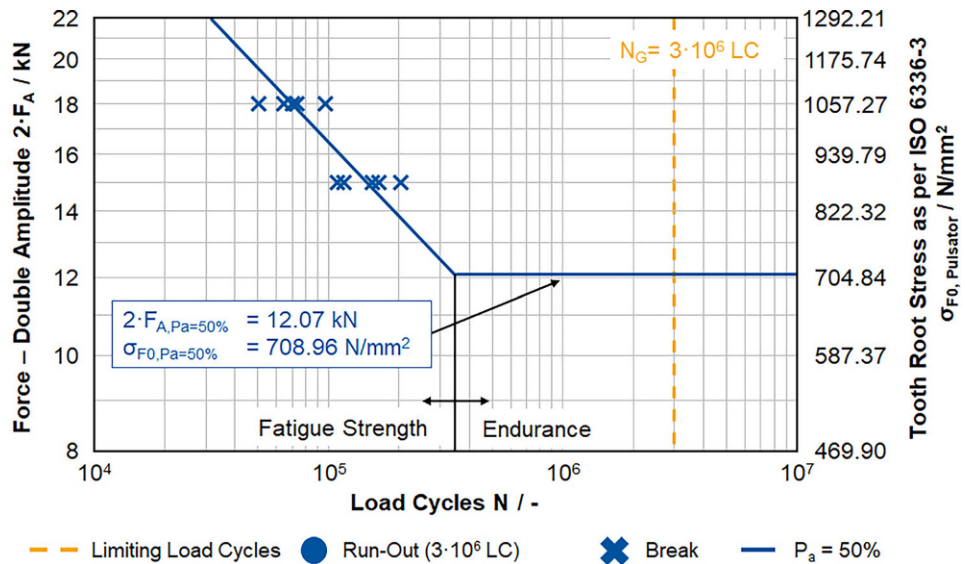


Fig. 8 SN-Curve of the 17-4PH gears ($\rho_{rel} = 99.0\%$)

load cycles N (X axis) into a suitable probability diagram, the best fit line for fatigue strength was created [22]. For the load level of the double amplitude of $2 \cdot F_{A,1} = 18$ kN, the probability of failure distribution $P_a = 50\%$ [29] was used determining the number of load cycles of $N_{50\%,1} = 69,444$ LC. Similarly, the number of load cycles for a load level of $2 \cdot F_{A,2} = 15$ kN was calculated to be $N_{50\%,2} = 145,925$ LC. The statistical evaluation of the test points in accordance with ROSSOW provided the supporting points for the fatigue strength line in the SN-curve, as shown in Fig. 8.

The SN-curve, which provides a connection between the load level of the double amplitude (Y axis) and the enduring number of load cycles N until fatigue damage

occurs (X axis), is only valid for the defined probability of failure $P_a = 50\%$. The intersection of the creep and fatigue lines was located at the double amplitude force of $2 \cdot F_{A,mean} = 12.07$ kN and the number of load cycles of $N_{50\%,SP} = 353,631$ LC. Furthermore, no pores were visible on the microscopic images of the fracture surfaces. Generally, it should be considered that the crack initiation, causing failure, was originated in the tooth root area on the surface of the 30° tangent.

To compare the tooth bending strength in the fatigue load range, the tooth root stresses of further tests on additional additively manufactured gear variants are shown in Fig. 9. The Y-axis shows the tooth root stress σ_{F0} calculated ac-

Test Conditions

- F_o = -0.5 kN
- F_u = variable
- F_A = variable
- f_{p4} \approx 153 Hz
- $z_{clamped}$ = 4
- P_a = 50 %
- T \approx RT (21°C)
- DR = Densification Rolling

Pulsator Test Rig

- P4: Electromagnetic Resonance Pulsator RUMUL TESTRONIC 150
- 17-4PH
- 17-4PH
- Screening
- 316L

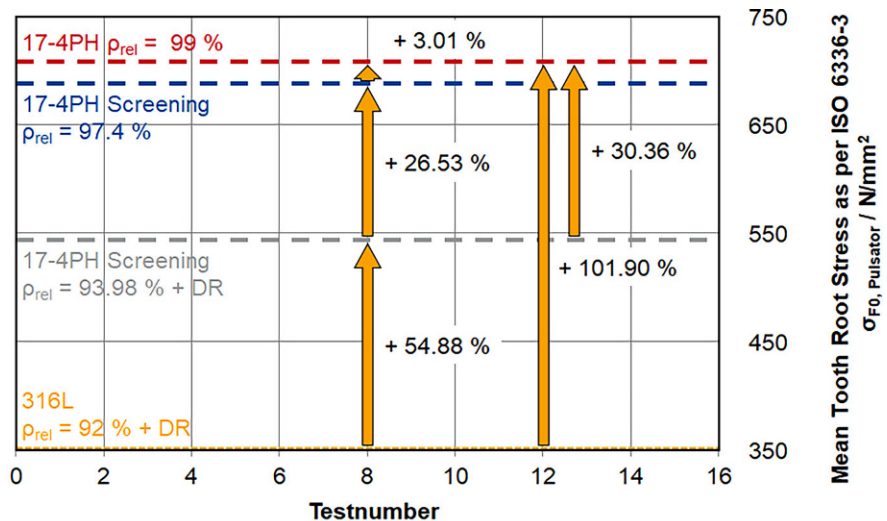
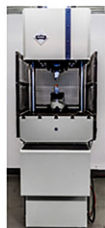


Fig. 9 Comparison of the tooth root stress of all gear variants

ording to ISO 6336 part 3 [17]. The tooth root stress is calculated as a function of the tooth root geometry. Ideally, the tooth root geometry of all variants is congruent, but slight deviations were still possible due to the process parameter settings. Therefore, a practical classification of all variants is not possible by the force of the double amplitude $2 \cdot F_A$. The tooth root stresses were calculated on the basis of the real tooth root radii. In addition to the investigations described in Chap. 2 for the tooth bending strength of the material 316L and the gears made of 17-4PH with a relative density of $\rho_{\text{rel}} = 97.4\%$, the calculated tooth bending strength of the optimized process variant with a relative density of $\rho_{\text{rel}} = 99.0\%$ and the tooth bending strength of a further variant ($\rho_{\text{rel}} = 93.98\%$) are shown as well.

The gears made of 17-4PH were manufactured with the process parameters derived in Chap. 2.2 and sintered by reducing the sintering temperature ($T_{\text{Sinter}} = 1280^\circ\text{C}$) to achieve a relative target density, i.e. the core density after the cold rolling process, of $\rho_{\text{rel}} = 93.98\%$. Although cold forming of the material 17-4PH is only possible in the annealed condition [26], the gears have been provided with a rolling stock allowance. As a result, the blanks do not feature an involute profile. Due to the densification of the surface zone by the rolling process, there is a density gradient from the surface to the core. The process parameters for cold rolling using the PROFIROLL PR 15HP rolling machine were adapted from KLEE [20]. During the rolling process, cracks occurred on the gears starting from the tip of the tooth. The cracks also spread on the tooth flank to a small extent. Due to the cracks, the gears were no longer usable. The cracks were caused by the material properties [26]. The mean value of the endurable double amplitude of the rolled gears with a relative density of

$\rho_{\text{rel}} = 93.98\%$ was $2 \cdot F_{A,\text{mean}} = 7.93\text{ kN}$, corresponding to an endurable tooth root stress of $\sigma_{F0} = 543.83\text{ N/mm}^2$.

The tests on the tooth bending strength of the variant with a relative density of $\rho_{\text{rel}} = 99.0\%$ showed a slight increase of $\Delta = 3.01\%$ in the fatigue strength of the gears compared to the gears tested in the screening tests ($\rho_{\text{rel}} = 97.4\%$). The increased bending strength is related to the process parameters set. In particular, the adjustment of the process parameters ensured that only flawless gears made of 17-4PH with a relative density of $\rho_{\text{rel}} = 99.0\%$ could be reproducibly and reliably produced. Compared to the screening tests of the rolled gears with a relative core density of $\rho_{\text{rel}} = 93.98\%$, an increase in bending strength of $\Delta = 30.36\%$ was achieved. In comparison with the results of the gears made of the material 316L, significant increases in bending strength were achieved for all 17-4PH variants. This is due to both the specific material properties and to the optimization of various process parameters, which are summarized in the following chapter.

6 Influences of relevant process parameters on component characteristics

The following chapter summarizes the optimized process parameters for the production of Binder Jetting gears made of 17-4PH stainless steel as well as the influences of the most relevant process parameters on the resulting component properties. The validation and evaluation of the process chain was conducted in terms of process reliability and reproducibility on the one hand and the achievable tooth bending strength on the other hand. An overview of the process parameters developed in Chap. 4 and the calculated tooth root stress σ_{F0} (described in Chap. 5) are shown in Fig. 10.

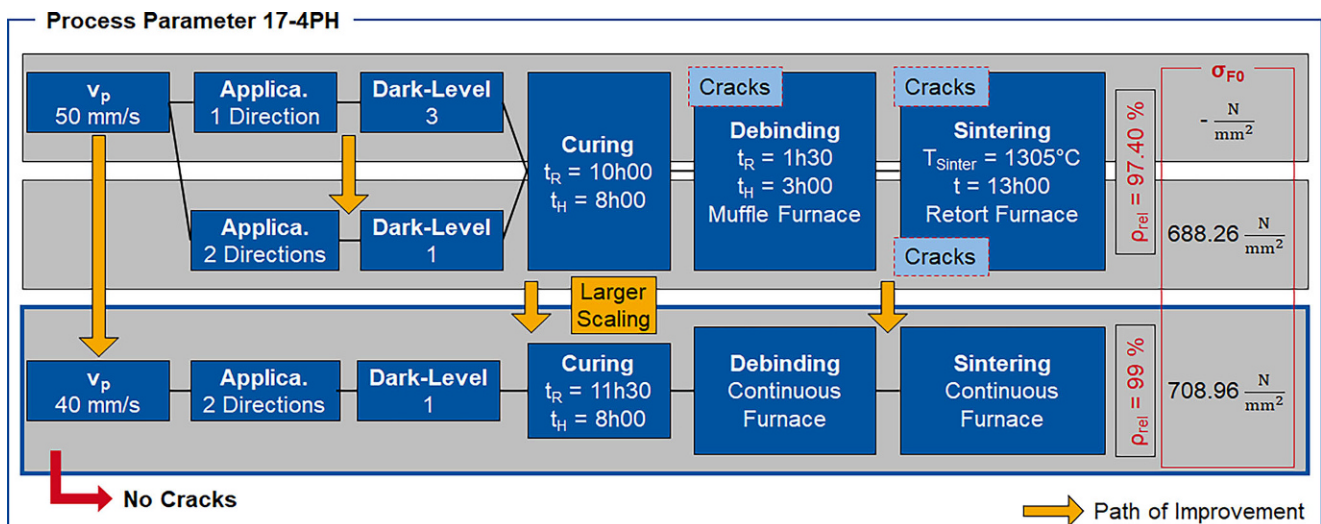


Fig. 10 Process Parameters of BJT Gear Manufacturing and the resulting Tooth Root Stress

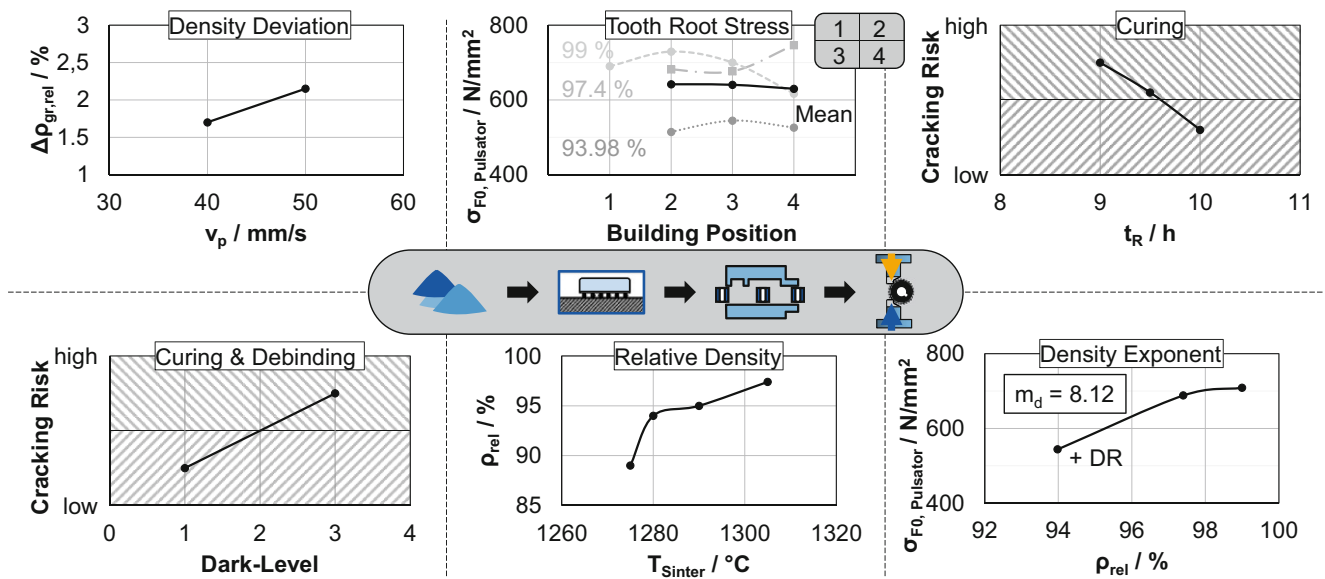


Fig. 11 Influences of relevant Process Parameters

Based on the process parameters described in Chap. 2.2 with a constant powder application speed of $v_p=50\text{mm/s}$ and two-sided powder application and a binder quantity of dark level 1 (66.67% of the maximum binder quantity that can be applied), further process adjustments were necessary due to crack formation after the sintering process, see lower part of Fig. 10. Due to the larger scaling of the gears and the resulting higher amount of binder applied, the ramp time for curing was extended accordingly to $t_R=11\text{h}30$. Both debinding and sintering took place in a continuous furnace. Sintering was realized at a sintering temperature of at least $T_{Sinter}=1305^\circ\text{C}$ over a total process time of $t=13\text{h}$. The effects of the main process parameters on the resulting gear properties are summarized in Fig. 11. Reducing the powder application speed v_p resulted in a more constant green density $\Delta\rho$ throughout the powder bed of the buildbox. Reducing the powder application speed by $\Delta v_p=10\text{mm/s}$ led to a decrease of the green density variation during the print from $\Delta\rho_{gr,rel}=2.2\%$ to $\Delta\rho_{gr,rel}=1.7\%$. This led to a decreasing risk of cracking on the one hand and an increasing component density on the other hand.

The position of the gear in the buildbox during the printing process only marginally influenced bending strength of the tooth (Fig. 11, top centre). After considering all the test points for each gear variant, an average tooth stress curve was determined. For position 1 in the buildbox, there were not enough data points for the relative densities of $\rho_{rel}=93.98\%$ and $\rho_{rel}=97.4\%$ to calculate a useful average. For positions 2, 3 and 4, there was no effect of the gear position on the tooth bending strength was detected. Extending the ramp time t_R during curing reduced the risk of cracking in the process. A ramp time of $t_R=10\text{h}$ was determined to be process reliable, depending on the green part

scaling. A lower (dark level 1) compared to a higher amount (dark level 3) of binder led to a reduced risk of cracking during debinding as well. A similar effect was registered during curing. However, reducing the amount of binder too much will result in an insufficient green strength of the gears. This has to be considered depending on the size of the component. A higher sintering temperature T_{Sinter} implies an increase in the relative density of the components ρ_{rel} after sintering. For the material 17-4PH, a minimum required sintering temperature of $T_{Sinter}=1305^\circ\text{C}$ was determined to achieve a relative density of $\rho_{rel}=99\%$. Higher tooth root capacities have also been achieved as a result of the increased gear density. Therefore, the objective of the process design of the Binder Jetting process chain for the production of 17-4PH gears with the highest possible tooth root load-bearing capacity is always aims to achieve a high relative component density.

7 Summary and outlook

In this report, the potential of gears manufactured by Binder Jetting (BJT), using the material 17-4PH (stainless steel X5CrNiCuNb16-4), has been analyzed with regard to the tooth bending strength. The relative density of the gears was increased up to $\rho_{0,rel}\approx 99\%$ by specific adjustment of the BJT process parameters. In addition, the reliability of the process and therefore the bending strength of the gears was increased as well. Both endurance and fatigue strength of 17-4PH BJT gears were investigated and the results were summarized in a SN-curve.

Different process variations along the process chain as well as their benefits were discussed [19]. The relative den-

sity of the gears made of the material 17-4PH after sintering was $\rho_{0,rel} \approx 97.4\%$ [19]. Despite the process modifications explained previously, some of the gears cracked depending on the furnace position after sintering. Based on the parameters determined by KLEE [19], further modifications to the process were required. Modifications were made to the powder application, the component scaling and thus the curing process as well as the debinding and sintering process. The previous occurrence of crack formations at some gears could result from variations in the relative green densities depending on the positioning in the buildbox. In general, a higher green density implies a lower shrinkage during sintering. This results in a reduction of the induced stresses and a reduced risk of crack formation. In addition to powder application in two directions of motion, the reduction of the powder application speed to $v_p = 40 \text{ mm/s}$ while keeping the layer thickness D_s constant lead to an increasing average green density by $\Delta\rho_{rel,m} = 2.4\%$. The average density of green compacts could be kept constant in the range of $\Delta\rho_{rel} = 1.7\%$ over all gear prints conducted. After sintering the gears, the geometric analysis revealed a partial undersize on the flanks and thus an insufficient grinding allowance. Therefore, the scaling factors of the printed gear were increased in X-, Y- and Z-direction ($\Delta = 3.43\%$) to prevent sintering shrinkage. The adjustment of the scaling factors leads to an increasing amount of binder and thus an extension of the curing time. The gears were debinded and sintered at identical process conditions [19] in a continuous furnace using a protective gas atmosphere (hydrogen H_2). After sintering, no visible damage or cracks at the gears were detected. 16 gears have been printed. All were completely undamaged, had sufficient oversize and a relative density of $\rho_{rel} = 99\%$. This value is higher than the value of the relative density of the variant tested in the screening trials [19]. The quality of the gears was measured after grinding using a gear measuring machine. All measured values averaged within quality class IT5 according to DIN EN ISO 1328 [7]. Subsequently, the tooth bending strength was tested on a pulsator test rig. The mean value of the endurable double amplitude ($N_G = 3 \cdot 10^6$ LC) was $2 \cdot F_{A,mean} = 12.07 \text{ kN}$, corresponding to an endurable tooth root stress of $\sigma_{F0} = 708.96 \text{ N/mm}^2$. The fatigue strength ($N_G < 3 \cdot 10^6$ LC) was determined according to the horizon method. The probability of failure was $P_a = 50\%$. The intersection of the creep and fatigue lines was located at the double amplitude force of $2 \cdot F_{A,mean} = 12.07 \text{ kN}$ and the number of load cycles of $N_{50\%,SP} = 353,631$ LC. The tests on the tooth bending strength of the variant with a relative density of $\rho_{rel} = 99.0\%$ showed a slight increase of $\Delta = 3.01\%$ in the fatigue strength of the gears compared to the gears tested in the screening tests ($\rho_{rel} = 97.4\%$). The increased bending strength is related to the process parameters set. In particular, the adjustment of the process

parameters ensured that only flawless gears made of 17-4PH with a relative density of $\rho_{rel} = 99.0\%$ could be reproducibly and reliably produced. Moreover, the endurance strength of cold rolled gears made of 17-4PH ($\rho_{0,rel} \approx 93.98\%$) was determined in screening tests. The mean value of the endurable double amplitude of the rolled gears with a relative density of $\rho_{rel} = 93.98\%$ was $2 \cdot F_{A,mean} = 7.93 \text{ kN}$, corresponding to an endurable tooth root stress of $\sigma_{F0} = 543.83 \text{ N/mm}^2$.

In short term, the influence of variable binder moistening and different relative densities on the mechanical properties will be investigated on bending and compressive specimens as an analogue sample to the gears. The validation will be realized by comparing the results to the bending strength results of the gears presented in this report. In long term, the development and certification of further materials, especially common gear steels such as 16MnCr5, is planned for the BJT.

Funding Open Access funding enabled and organized by Projekt DEAL.

Open Access This article is licensed under a Creative Commons Attribution 4.0 International License, which permits use, sharing, adaptation, distribution and reproduction in any medium or format, as long as you give appropriate credit to the original author(s) and the source, provide a link to the Creative Commons licence, and indicate if changes were made. The images or other third party material in this article are included in the article's Creative Commons licence, unless indicated otherwise in a credit line to the material. If material is not included in the article's Creative Commons licence and your intended use is not permitted by statutory regulation or exceeds the permitted use, you will need to obtain permission directly from the copyright holder. To view a copy of this licence, visit <http://creativecommons.org/licenses/by/4.0/>.

References

1. AKSteel (2007) Data sheet 420 stainless steel
2. Andersen O, Studnitzky T, Hein S, Riecker S, Quadbeck P, Petzold F, Kieback B (2018) Neue Entwicklungen auf dem Gebiet der nicht-strahlbasierten additiven Fertigungsverfahren. In: Tagungsband zur Hagen, 29./30. November. Dortmund: Heimdall, pp 255–280
3. Beiss P (2013) Pulvermetallurgische Fertigungstechnik, 1st edn. Springer, Berlin, Heidelberg
4. Bergs T, Brimmers J, Klee L (2020) Binder jetting. PM gears in small series production. In: Müller B (ed) Fraunhofer Direct Digital Manufacturing Conference DDMC 2020. Fraunhofer, Stuttgart
5. Brecher C (2011) Integrative Produktionstechnik für Hochlohnländer. Springer, Berlin
6. Digital Metal (2020) DM P2500 Data Sheet
7. Norm ISO 1328 Teil 1 (September 2013) Cylindrical gears. ISO system of flank tolerance classification. Definitions and allowable values of deviations relevant to flanks of gear teeth
8. DIN EN 10088-1 (Dezember 2014) DIN EN 10088-1: Nichtrostende Stähle
9. Norm DIN EN ISO / ASTM 52900 (Juni 2017) Additive Fertigung – Grundlagen – Terminologie

10. Norm DIN EN ISO 21920-3 (Dezember 2022) Geometrische Produktspezifikation (GPS) Oberflächenbeschaffenheit: Profile – Teil 3: Spezifikationsoperatoren
11. Dixon W, Mood A (1948) A method for obtaining and analyzing sensitivity data. *J Am Stat Assoc* 241(43):109–126
12. Dutta B (2019) *Science, technology and applications of metals in additive manufacturing*. Elsevier, Amsterdam
13. Haberhauer H (2018) *Maschinenelemente. Gestaltung, Berechnung, Anwendung*, 18th edn. Springer, Berlin, Heidelberg
14. Haibach E (2006) *Betriebsfestigkeit. Verfahren und Daten zur Bauteilberechnung*, 3rd edn. Springer, Berlin
15. Höganäs Group Company (Digital Metal) (2020) *Materials for 3D printing*. Höganäs
16. Hück M (1983) Ein verbessertes Verfahren für die Auswertung von Treppenstufenversuchen. *Werkstattstech Online* 24:406–417
17. ISO 6336-3 (November 2019) ISO 6336-3: Calculation of load capacity of spur and helical gears—Part 3
18. Issler L, Ruoß H, Häfele P (2006) *Festigkeitslehre – Grundlagen*, 2nd edn. Springer, Berlin, Heidelberg
19. Klee L, Brimmers J, Bergs T (2022) Tooth root load capacity of additive manufactured gears. In: Brecher C, Bergs T (eds) 9th WZL Gear Conference USA. Elgin, IL/ USA: Reishauer USA, July 21st/ 22nd 2022, pp 3–1–3–19
20. Klee L, Brimmers J, Bergs T (2023) Potential of densified binder jetting gears regarding tooth root load capacity. In: Müller B (ed) *Fraunhofer Direct Digital Manufacturing Conference DDMC 2023*. Fraunhofer, Stuttgart
21. Klocke F (2015) *Gießen, Pulvermetallurgie, Additive Manufacturing*, 4th edn. *Fertigungsverfahren*, vol 5. Springer, Berlin
22. Klocke F, Brecher C (2017) *Zahnrad- und Getriebetechnik. Auslegung – Herstellung – Untersuchung – Simulation*, 1st edn. Hanser, München
23. Kotthoff G (2003) *Neue Verfahren zur Tragfähigkeitssteigerung von gesinterten Zahnradern*. Diss. RWTH Aachen University
24. Mandt D (2006) *Eigenschaften und Einsatzverhalten von leichten und dämpfenden Werkstoffverbund-Zahnradern*. Diss. RWTH Aachen University
25. Rossow E (1964) Eine einfache Rechenschiebernäherung an die den Normal Scores entsprechenden Prozentpunkte. *Qualitätskontrolle* 9:146–147
26. Sandmeyer Steel Company (2018) *Datenblatt 17-4PH*
27. Schlecht B (2010) *Getriebe – Verzahnungen – Lager. Maschinenelemente*, vol 2. Pearson Studium, München
28. Verband Deutscher Maschinen- und Anlagenbau e.V. (2018) *Antrieb im Wandel. Die Elektrifizierung des Antriebsstrangs von Fahrzeugen und ihre Auswirkung auf den Maschinen- und Anlagenbau und die Zulieferindustrie*
29. Zenner H, Mauch H (1999) *Statistische Methoden zur Beurteilung von Bauteillebensdauer und Zuverlässigkeit und ihre beispielhafte Anwendung auf Zahnradern – Leitfaden zur Statistik in der Betriebsfestigkeit*. Informationsblatt zum Forschungsvorhaben, vol 304/I. Forschungsvereinigung Antriebstechnik e. V.